Huerta, A., Vidal, Y. and Villon, P., Pseudo-divergence-free element free Galerkin method for incompressible fluid flow, *Computer Methods in Applied Mechanics and Engineering,* Vol. 193, Issue 12 - 14, pp. 1119-1136, 2004

Pseudo-divergence-free element free Galerkin method for incompressible fluid flow ⋆

Antonio HUERTA [a,1], Yolanda VIDAL [a] and Pierre VILLON [b]

[a] *Laboratori de Càlcul Numèric, Universitat Politècnica de Catalunya, Jordi Girona 1, E-08034 Barcelona, Spain.*

[b] *Laboratoire de Mécanique Roberval, UMR UTC-CNRS Université de Technologie de Compiègne, BP 20529, 60205 Compiègne cedex, France.*

Abstract

Incompressible modelling in finite elements has been a major concern since its early developments and has been extensively studied. However, incompressibility in mesh-free methods is still an open topic. Thus, instabilities or locking can preclude the use of mesh-free approximations in such problems. Here, a novel mesh-free formulation is proposed for incompressible flow. It is based on defining a pseudo-divergence-free interpolation space. That is, the finite dimensional interpolation space approaches a divergence-free space when the discretization is refined. Note that such an interpolation does not include any overhead in the computations. The numerical evaluations are performed using the inf-sup numerical test and two well-known benchmark examples for Stokes flow.

Key words: Locking, Element Free Galerkin, Diffuse derivatives, Moving Least Squares, Incompressible flow, LBB condition

1 Introduction

Accurate and efficient modeling of incompressible flows is an important issue in finite elements. The continuity equation for an incompressible fluid takes

⋆ Research supported by Ministerio de Ciencia y Tecnología under grants DPI2001-2204 and REN2001-0925-C03-01

Email address: antonio.huerta@upc.es (Antonio HUERTA).
URL: www-lacan.upc.es (Antonio HUERTA).

[1] Correspondence to: Antonio Huerta, Departament de Matemàtica Aplicada III, E.T.S. de Ingenieros de Caminos, Canales y Puertos, Universitat Politècnica de Catalunya, Jordi Girona 1, E-08034 Barcelona, SPAIN.

the peculiar form. It consists of a constraint on the velocity field that must be divergence free. Then, the pressure has to be considered as a variable not related to any constitutive equation. Its presence in the momentum equation has the purpose of introducing an additional degree of freedom needed to satisfy the incompressibility constraint. The role of the pressure variable is thus to adjust itself instantaneously in order to satisfy the condition of divergence-free velocity. That is, the pressure is acting as a Lagrangian multiplier of the incompressibility constraint and thus there is a coupling between the velocity and the pressure unknowns.

Various formulations have been proposed in the literature to deal with incompressible flow problems [1–8]. Mixed finite elements present numerical difficulties caused by the saddle-point nature of the resulting variational problem. Solvability of the problem depends on a proper choice of finite element spaces for velocity and pressure. They must satisfy a compatibility condition, the so-called LBB (or inf-sup) condition. If this is not the case, alternative formulations (usually depending on a numerical parameter) are devised to circumvent the LBB condition and enable the use of velocity–pressure pairs that are unstable in the standard Galerkin formulation. Finally, note that it is not trivial to verify analytically the LBB condition for a given interpolation of velocity and pressure, and this has spurred the use of numerical inf-sup testing [9–12].

Incompressibility in mesh-free methods is still an open topic. Even recently, it was claimed [13] that meshless methods do not exhibit volumetric locking. Now it is clear that this is not true. For instance, an analysis of the element free Galerkin (EFG) method using the numerical inf-sup condition can be found in [14]. Moreover, several authors claim that increasing the dilation parameter locking phenomena in mesh-free methods can be suppressed, or at least attenuated. Their argument is based on numerical examples [15,14] or on the heuristic constraint ratio [16] proposed in [17]. In a recent paper [18] this issue is clarified determining the influence of the dilation parameter on the locking behavior of EFG near the incompressible limit. This is done performing a modal analysis: studying the fundamental modes (base of the solution space) and their corresponding energy (eigenvalue). In particular EFG behavior is compared with standard finite elements. The major conclusion is that an increase of the dilation parameter attenuates, but *never suppresses* the volumetric locking and that, as in standard finite elements, an increase in the order of reproducibility reduces the relative number of locking modes at a lower rate than finite elements.

Until now remedies proposed in the literature are extensions of methods developed for finite elements. For instance, in [14] a new EFG formulation is proposed using selective reduced integration and in [16] an improved Reproducing Kernel Particle Method based on a pressure projection method is suggested.

Here a novel approach is explored: the pseudo-divergence-free (PDF) EFG method. It consists in using interpolation functions that verify approximately the divergence-free constraint for a given discretization, and asymptotically become divergence-free as the discretization is refined. This method is based on diffuse derivatives [19], which, as proven in [20], converge to the derivatives of the exact solution when the radius of the support goes to zero (for a fixed dilation parameter). One of the key advantages of this approach is that the pseudo-divergence-free (PDF) interpolation functions are computed *a priori*. That is, prior to determining the specific particle distribution. Thus, there is no extra computational cost.

Preliminary results (modal analysis) in incompressible elasticity were encouraging [21,22]. In this paper convergence of the approximation in incompressible flows is studied. In particular, it is shown that the PDF EFG method passes the numerical inf-sup test. And two well-known examples of Stokes flow are used to compare different mixed formulations.

2 Diffuse derivatives

2.1 Preliminaries of the EFG method

This section will not be devoted to develop or discuss mesh-free methods in detail or their relation with moving least squares (MLS) interpolants. There are well known references with excellent presentations of mesh-free methods. See, for instance, the papers in the special issue [23]. Here some basic notions will be recalled in order to introduce the notation and the approach employed in following sections.

The moving least squares approach is based on the local approximation (i.e., at any point $\boldsymbol{z}$ in the neighborhood of $\boldsymbol{x}$) of the unknown scalar function $u(\boldsymbol{z})$ by u^ρ as

$$u(\boldsymbol{z}) \simeq u^\rho(\boldsymbol{x},\boldsymbol{z}) = \mathbf{P}^\mathsf{T}(\boldsymbol{z})\ \mathbf{a}(\boldsymbol{x}) \qquad \text{for } \boldsymbol{z} \text{ near } \boldsymbol{x}, \tag{1}$$

where the coefficients $\mathbf{a}(\boldsymbol{x}) = \{\mathrm{a}_0(\boldsymbol{x}), \mathrm{a}_1(\boldsymbol{x}), \ldots, \mathrm{a}_l(\boldsymbol{x})\}^\mathsf{T}$ are not constant, they depend on point $\boldsymbol{x}$, and $\mathbf{P}(\boldsymbol{z}) = \{p_0(\boldsymbol{z}), p_1(\boldsymbol{z}), \ldots, p_l(\boldsymbol{z})\}^\mathsf{T}$ includes a complete basis of the subspace of polynomials of degree m. In one dimension, it is usual that $p_i(x)$ coincides with the monomials x^i, and, in this particular case, $l = m$. The coefficients $\mathbf{a}$ are obtained by minimization of the functional $J_{\boldsymbol{x}}(\mathbf{a})$ centered in $\boldsymbol{x}$ and defined by

$$J_{\boldsymbol{x}}(\mathbf{a}) = \sum_{i\in I_{\boldsymbol{x}}} \phi(\boldsymbol{x},\boldsymbol{x}_i)\Big[u(\boldsymbol{x}_i) - \mathbf{P}^\mathsf{T}(\boldsymbol{x}_i)\ \mathbf{a}(\boldsymbol{x})\Big]^2, \tag{2}$$

where $\phi(\boldsymbol{x},\boldsymbol{x}_i)$ is a weighting function (positive, even and with compact support) that characterizes the mesh-free method. For instance, if $\phi(\boldsymbol{x},\boldsymbol{x}_i)$ is con-

tinuous together with its first k derivatives, the interpolation is also continuous together with its first k derivatives. The particles cover the computational domain Ω, $\Omega \subset \mathbb{R}^{\mathtt{n_{sd}}}$, and, in particular, a number of particles $\{\boldsymbol{x}_i\}_{i\in I_{\boldsymbol{x}}}$ belong to the support of $\phi(\boldsymbol{x},\boldsymbol{x}_i)$. The minimization of $J_{\boldsymbol{x}}(\mathbf{a})$ induces the standard normal equations in a weighted least-squares problem

$$\mathbf{M}(\boldsymbol{x})\ \mathbf{a}(\boldsymbol{x}) = \sum_{i\in I_{\boldsymbol{x}}} \phi(\boldsymbol{x},\boldsymbol{x}_i)\ \mathbf{P}(\boldsymbol{x}_i)\ u(\boldsymbol{x}_i) \tag{3}$$

where, as usual, the Gram matrix $\mathbf{M}(\boldsymbol{x})$ is the scalar product of the interpolation polynomials:

$$\mathbf{M}(\boldsymbol{x}) = \sum_{i\in I_{\boldsymbol{x}}} \phi(\boldsymbol{x},\boldsymbol{x}_i)\ \mathbf{P}(\boldsymbol{x}_i)\ \mathbf{P}^{\mathsf{T}}(\boldsymbol{x}_i).$$

That is,

$$\langle u, v\rangle_{\boldsymbol{x}}\ = \sum_{i\in I_{\boldsymbol{x}}} \phi(\boldsymbol{x},\boldsymbol{x}_i)\ u(\boldsymbol{x}_i)\ v(\boldsymbol{x}_i) \tag{4}$$

must define a discrete scalar product. Thus, several conditions on the particle distribution are implicitly assumed, see for instance [24,25].

Once the normal equations, Eqs (3), are solved the coefficients $\mathbf{a}$ are substituted in (1). Since the weighting function ϕ usually favors the central point $\boldsymbol{x}$, it seems reasonable to assume that such an approximation is more accurate precisely at $\boldsymbol{z} = \boldsymbol{x}$ and thus the approximation (1) is particularized at $\boldsymbol{x}$, that is,

$$u(\boldsymbol{x}) \simeq u^{\rho}(\boldsymbol{x}) = \mathbf{P}^{\mathsf{T}}(\boldsymbol{x})\ \mathbf{a}(\boldsymbol{x}) = \mathbf{P}^{\mathsf{T}}(\boldsymbol{x})\ \mathbf{M}^{-1}(\boldsymbol{x}) \sum_{i\in I_{\boldsymbol{x}}} \phi(\boldsymbol{x},\boldsymbol{x}_i)\ \mathbf{P}(\boldsymbol{x}_i)\ u(\boldsymbol{x}_i). \tag{5}$$

This expression can also be written in a standard interpolation form

$$u^{\rho}(\boldsymbol{x}) = \sum_{i\in I_{\boldsymbol{x}}} N_i^{\rho}(\boldsymbol{x})\ u(\boldsymbol{x}_i) = \sum_{i\in I_{\boldsymbol{x}}} \underbrace{\Big[\phi(\boldsymbol{x},\boldsymbol{x}_i)\ \mathbf{P}^{\mathsf{T}}(\boldsymbol{x})\ \mathbf{M}^{-1}(\boldsymbol{x})\ \mathbf{P}(\boldsymbol{x}_i)\Big]}_{N_i^{\rho}(\boldsymbol{x})}\ u(\boldsymbol{x}_i). \tag{6}$$

2.2 The diffuse derivative

The approximation of the derivative of u in each spatial direction is the corresponding derivative of u^{ρ}. This requires to derive (5), that is

$$\frac{\partial u}{\partial \boldsymbol{x}} \simeq \frac{\partial u^{\rho}}{\partial \boldsymbol{x}} = \frac{\partial \mathbf{P}^{\mathsf{T}}}{\partial \boldsymbol{x}}\ \mathbf{a} + \mathbf{P}^{\mathsf{T}}\ \frac{\partial \mathbf{a}}{\partial \boldsymbol{x}}. \tag{7}$$

On one hand, the second term on the r.h.s. is not trivial. Derivatives of the coefficients $\mathbf{a}$ require the resolution of a linear system of equations with the

same matrix $\mathbf{M}$. As noted in [26] this is not an expensive task. However, it requires the knowledge of the cloud of particles surrounding each point $\boldsymbol{x}$, and, thus, it depends on the point where derivatives are evaluated.

On the other hand, the first term is easily evaluated. The derivative of the polynomials in $\mathbf{P}$ is trivial and can be evaluated *a priori*, without knowledge of the cloud of particles surrounding each point $\boldsymbol{x}$.

The concept of diffuse derivative proposed in [20,19] consist in approximating the derivative only with the first term on the r.h.s. of (7), namely

$$\frac{\delta u^\rho}{\delta \boldsymbol{x}} = \left.\frac{\partial u^\rho}{\partial \boldsymbol{z}}\right|_{\boldsymbol{z}=\boldsymbol{x}} = \left.\frac{\partial \mathbf{P}^\mathsf{T}}{\partial \boldsymbol{z}}\right|_{\boldsymbol{z}=\boldsymbol{x}} \mathbf{a}(\boldsymbol{x}) = \frac{\partial \mathbf{P}^\mathsf{T}}{\partial \boldsymbol{x}}\,\mathbf{a}(\boldsymbol{x}).$$

From a computational cost point of view, this is an interesting alternative to (7). Moreover, in [20] it is shown that the diffuse derivative converges at optimal rate to the derivative of u, here the proof is developed in several spatial dimensions.

Proposition 1 *If u^ρ is an approximation to u with an order of consistency m (i.e., $\mathbf{P}$ includes a complete basis of the subspace of polynomials of degree m) and ρ/h is constant, then*

$$\left\| \frac{\partial^{|\boldsymbol{k}|} u}{\partial \boldsymbol{x}^{\boldsymbol{k}}} - \frac{\delta^{|\boldsymbol{k}|} u^\rho}{\delta \boldsymbol{x}^{\boldsymbol{k}}} \right\|_\infty \leq C(\boldsymbol{x}) \frac{\rho^{m+1-|\boldsymbol{k}|}}{(m+1)!} \qquad \forall |\boldsymbol{k}| = 0, \ldots, m. \tag{8}$$

where $\boldsymbol{k}$ is a multi-index, $\boldsymbol{k} = (k_1, k_2, \ldots, k_{n_{sd}})$ and $|\boldsymbol{k}| = k_1 + k_2 + \cdots + k_{n_{sd}}$.

Proof. Lets assume $u \in \mathcal{C}^{m+1}(\overline{\Omega})$ where $\mathcal{C}^{m+1}$ is the space of $(m+1)$ times continuously differentiable functions. Recall that Taylor's formula of order m can be written as:

$$u(\boldsymbol{x}+\boldsymbol{h}) = \sum_{|\boldsymbol{\alpha}|=0}^{m} \frac{1}{\alpha!} \boldsymbol{h}^\alpha \frac{\partial^{|\boldsymbol{\alpha}|} u}{\partial \boldsymbol{x}^{\boldsymbol{\alpha}}}(\boldsymbol{x}) + R^\star_{m+1}(\boldsymbol{x}+\theta\boldsymbol{h}), \tag{9}$$

where $\theta \in]0,1[$, $R^\star_{m+1}(\boldsymbol{x}+\theta\boldsymbol{h})$ is the error term and $\boldsymbol{\alpha}$ is a multi-index such that,

$$\boldsymbol{h}^\alpha := h_1^{\alpha_1} h_2^{\alpha_2} \cdots h_{\mathtt{n_{sd}}}^{\alpha_{\mathtt{n_{sd}}}}; \quad \boldsymbol{\alpha}! := \alpha_1! \alpha_2! \cdots \alpha_{\mathtt{n_{sd}}}!; \quad |\boldsymbol{\alpha}| = \alpha_1 + \alpha_2 + \cdots + \alpha_{\mathtt{n_{sd}}}.$$

Without loss of generality, the definitions $\boldsymbol{z} := \boldsymbol{x} + \boldsymbol{h}$ and

$$R_{m+1}(\boldsymbol{x}, \boldsymbol{z}) := R^\star_{m+1}\Big(\boldsymbol{x} + \theta(\boldsymbol{z} - \boldsymbol{x})\Big) \tag{10}$$

allow us to rewrite equation (9) as

$$u(\boldsymbol{z}) = \sum_{|\boldsymbol{\alpha}|=0}^{m} \frac{1}{\boldsymbol{\alpha}!} \left(\frac{\boldsymbol{z}-\boldsymbol{x}}{\rho} \right)^{\alpha} \rho^{\alpha} \frac{\partial^{|\boldsymbol{\alpha}|} u}{\partial \boldsymbol{x}^{\boldsymbol{\alpha}}}(\boldsymbol{x}) + R_{m+1}(\boldsymbol{x}, \boldsymbol{z}),$$

where, as usual, the dependence of θ in $\boldsymbol{x}$ and $\boldsymbol{z}$ is not explicitly stated. Thus, Taylor's formula can also be written as:

$$u(\boldsymbol{z}) = \mathbf{P}^{\mathsf{T}}\Big(\frac{\boldsymbol{z}-\boldsymbol{x}}{\rho} \Big) \mathbf{U}(\boldsymbol{x}) + R_{m+1}(\boldsymbol{x}, \boldsymbol{z}), \tag{11}$$

where each component of $\mathbf{P}$ and $\mathbf{U}$ is defined, respectively, by

$$\mathrm{P}_{\boldsymbol{\alpha}}(\boldsymbol{\xi}) = \frac{\boldsymbol{\xi}^{\boldsymbol{\alpha}}}{\alpha!} \quad \text{and} \quad \mathrm{U}_{\boldsymbol{\alpha}}(\boldsymbol{x}) = \rho^{\boldsymbol{\alpha}} \frac{\partial^{|\boldsymbol{\alpha}|} u}{\partial \boldsymbol{x}^{\boldsymbol{\alpha}}} \quad \text{for } |\boldsymbol{\alpha}| = 0, \ldots, m. \tag{12}$$

Observe that $\mathbf{U}(\boldsymbol{x})$ depends on the exact derivatives of u.

The MLS approach is based on the local approximation of the unknown scalar function u by u^{ρ}, see equation (1). Since in equation (11) polynomials $\mathbf{P}(\xi)$ are centered and scaled, the MLS interpolant is also centered and scaled,

$$u(\boldsymbol{z}) \simeq u^{\rho}(\boldsymbol{x}, \boldsymbol{z}) = \mathbf{P}^{\mathsf{T}}\Big(\frac{\boldsymbol{z}-\boldsymbol{x}}{\rho} \Big)\, \mathbf{a}(\boldsymbol{x}) \qquad \text{for } \boldsymbol{z} \text{ near } \boldsymbol{x}.$$

Then the MLS approach requires the resolution of the normal equations given by (3); here $u(\boldsymbol{x}_i)$ is substituted using (11) and the scalar product defined in (4) is employed to simplify the notation,

$$\mathbf{M}(\boldsymbol{x})\, \mathbf{a}(\boldsymbol{x}) = \left\langle \mathbf{P}\Big(\frac{\boldsymbol{z}-\boldsymbol{x}}{\rho} \Big), \mathbf{P}^{\mathsf{T}}\Big(\frac{\boldsymbol{z}-\boldsymbol{x}}{\rho} \Big) \mathbf{U}(\boldsymbol{x}) + R_{m+1}(\boldsymbol{x}, \boldsymbol{z}) \right\rangle_{\boldsymbol{x}}.$$

This equation can be rearranged as

$$\mathbf{M}(\boldsymbol{x})[\mathbf{a}(\boldsymbol{x}) - \mathbf{U}(\boldsymbol{x})] = \sum_{j \in I_{\boldsymbol{x}}} \phi\Big(\frac{\boldsymbol{x}_j - \boldsymbol{x}}{\rho} \Big) \mathbf{P}\Big(\frac{\boldsymbol{x}_j - \boldsymbol{x}}{\rho} \Big) R_{m+1}(\boldsymbol{x}, \boldsymbol{x}_j) =: \mathbf{b}. \tag{13}$$

Now, lets rewrite the r.h.s. of (13) in a more convenient way. The error term of Taylor's formula has the form

$$R_{m+1}(\boldsymbol{x}, \boldsymbol{x}_j) = \sum_{|\boldsymbol{\alpha}|=m+1} \frac{(\boldsymbol{x}_j - \boldsymbol{x})^{\boldsymbol{\alpha}}}{(m+1)!} \frac{\partial^{m+1} u}{\partial \boldsymbol{x}^{\alpha}}(\boldsymbol{x}, \boldsymbol{x}_j), \tag{14}$$

where, as in equation (10), the intermediate point θ is not explicitly stated but its dependence on $\boldsymbol{x}$ and $\boldsymbol{x}_j$ is reflected. Substituting (14) in the definition of vector $\mathbf{b}$, see (13), produces

$$\mathbf{b} = \sum_{j \in I_{\boldsymbol{x}}} \phi\Big(\frac{\boldsymbol{x}_j - \boldsymbol{x}}{\rho} \Big) \mathbf{P}\Big(\frac{\boldsymbol{x}_j - \boldsymbol{x}}{\rho} \Big) \sum_{|\boldsymbol{\alpha}|=m+1} \frac{(\boldsymbol{x}_j - \boldsymbol{x})^{\boldsymbol{\alpha}}}{(m+1)!} \frac{\partial^{m+1} u}{\partial \boldsymbol{x}^{\alpha}}(\boldsymbol{x}, \boldsymbol{x}_j).$$

Each component of the previously defined vector $\mathbf{b}$ is associated to the corresponding component of $\mathbf{P}$, namely the polynomial of degree $|\boldsymbol{k}| = 0, \dots, m$ defined as

$$\xi^{\boldsymbol{k}}/\boldsymbol{k}! = \left(\xi_1^{k_1}\xi_2^{k_2}\cdots\xi_{\mathtt{n_{sd}}}^{k_{\mathtt{n_{sd}}}}\right)/\left(k_1!k_2!\cdots k_{\mathtt{n_{sd}}}!\right).$$

Under these circumstances, each component of $\mathbf{b}$ can be written as

$$\begin{aligned} b_{\boldsymbol{k}} &= \sum_{j\in I_{\boldsymbol{x}}} \phi\Big(\frac{\boldsymbol{x}_j-\boldsymbol{x}}{\rho}\Big)\frac{(\boldsymbol{x}_j-\boldsymbol{x})^{\boldsymbol{k}}}{\rho^{|\boldsymbol{k}|}}\frac{1}{|\boldsymbol{k}|!}\sum_{|\alpha|=m+1}\frac{(\boldsymbol{x}_j-\boldsymbol{x})^{\alpha}}{(m+1)!}\frac{\partial^{m+1}u}{\partial\boldsymbol{x}^{\boldsymbol{\alpha}}}(\boldsymbol{x},\boldsymbol{x}_j) \\ &= \frac{\rho^{m+1}}{(m+1)!}\underbrace{\frac{1}{|\boldsymbol{k}|!}\sum_{j\in I_{\boldsymbol{x}}}\phi\Big(\frac{\boldsymbol{x}_j-\boldsymbol{x}}{\rho}\Big)\sum_{|\boldsymbol{\alpha}|=m+1}\Big(\frac{\boldsymbol{x}_j-\boldsymbol{x}}{\rho}\Big)^{\boldsymbol{k}+\boldsymbol{\alpha}}\frac{\partial^{m+1}u}{\partial\boldsymbol{x}^{\alpha}}(\boldsymbol{x},\boldsymbol{x}_j)}_{r_{\boldsymbol{k}}(\boldsymbol{x})} \\ &= \frac{\rho^{m+1}}{(m+1)!}r_{\boldsymbol{k}}(\boldsymbol{x}). \end{aligned} \tag{15}$$

Thus, the r.h.s. of (13) becomes

$$\mathbf{b} = \frac{\rho^{m+1}}{(m+1)!}\,\mathbf{r}(\boldsymbol{x}). \tag{16}$$

Substituting (16) into equation (13) and assuming that $\mathbf{M}$ is regular [24,25],

$$\mathbf{a}(\boldsymbol{x}) - \mathbf{U}(\boldsymbol{x}) = \frac{\rho^{m+1}}{(m+1)!}\,\mathbf{M}^{-1}(\boldsymbol{x})\;\mathbf{r}(\boldsymbol{x}).$$

On one hand, $r_{\boldsymbol{k}}$ is bounded for all $|\boldsymbol{k}| = 0, \dots, m$. This can be seen from the definition of $r_{\boldsymbol{k}}$, see (15). Note that for a fixed $\boldsymbol{x}$, if ρ/h is constant, $r_{\boldsymbol{k}}$ is the sum of products of continuous functions in Ω. Thus, it is a continuous function in Ω. Moreover, in every product, there is the weighting function ϕ, which has compact support. Since $r_{\boldsymbol{k}}$ is a continuous function with compact support it is bounded by a constant that only depends on $\boldsymbol{x}$.

On the other hand, matrix $\mathbf{M}$ is also bounded [27,25]. Then, if both, $\mathbf{M}$ and $r_{\boldsymbol{k}}$, are bounded, a constant $C(\boldsymbol{x})$ can be defined as the bound of $\mathbf{M}^{-1}(\boldsymbol{x})\mathbf{r}(\boldsymbol{x})$ and consequently

$$|\mathbf{a}(\boldsymbol{x}) - \mathbf{U}(\boldsymbol{x})| \le \frac{\rho^{m+1}}{(m+1)!}\,C(\boldsymbol{x})$$

The previous expression can be divided by $\rho^{|\boldsymbol{k}|}$. Then, for each component,

$$\left|\frac{\mathrm{a}_{\boldsymbol{k}}(\boldsymbol{x})}{\rho^{|\boldsymbol{k}|}} - \frac{\mathrm{U}_{\boldsymbol{k}}(\boldsymbol{x})}{\rho^{|\boldsymbol{k}|}}\right| \le \frac{\rho^{m+1-|\boldsymbol{k}|}}{(m+1)!}\,C(\boldsymbol{x}) \qquad \forall\,|\boldsymbol{k}| = 0,\dots,m, \tag{17}$$

where $\mathrm{a}_{\boldsymbol{k}}$ and $\mathrm{U}_{\boldsymbol{k}}$ are the components of $\mathbf{a}$ and $\mathbf{U}$, respectively. Recall that each component of $\mathbf{U}(\boldsymbol{x})$ depends on the corresponding exact derivatives of u, see (12). Now, observe that each component of $\mathbf{a}(\boldsymbol{x})$ shall depend on the

corresponding pseudo-derivatives; that is, for $|\boldsymbol{k}| = 0, ..., m$

$$\frac{\delta^{|\boldsymbol{k}|}u^\rho}{\delta \boldsymbol{x}^{\boldsymbol{k}}} := \frac{\delta^{|\boldsymbol{k}|}u^\rho}{\delta x_1^{\boldsymbol{k}_1}\cdots\delta x_{\mathtt{n_{sd}}}^{\boldsymbol{k}_{\mathtt{n_{sd}}}}} := \left.\frac{\partial^{|\boldsymbol{k}|}u^\rho}{\partial z_1^{\boldsymbol{k}_1}\cdots\partial z_{\mathtt{n_{sd}}}^{\boldsymbol{k}_{\mathtt{n_{sd}}}}}\right|_{\boldsymbol{z}=\boldsymbol{x}} = \frac{\mathrm{a}_{\boldsymbol{k}}(\boldsymbol{x})}{\rho^{\boldsymbol{k}_1}\cdots\rho^{\boldsymbol{k}_{\mathtt{n_{sd}}}}}. \tag{18}$$

Finally, replacing the definition of $\mathbf{U}(\boldsymbol{x})$ and $\mathbf{a}(\boldsymbol{x})$ given by (12) and (18) in (17), one gets the final expression, which completes the proof,

$$\left\| \frac{\partial^{|\boldsymbol{k}|}u}{\partial \boldsymbol{x}^{\boldsymbol{k}}} - \frac{\delta^{|\boldsymbol{k}|}u^\rho}{\delta \boldsymbol{x}^{\boldsymbol{k}}} \right\|_\infty \leq C(\boldsymbol{x})\frac{\rho^{m+1-|\boldsymbol{k}|}}{(m+1)!} \qquad \forall |\boldsymbol{k}| = 0, \ldots, m. \qquad \square$$

3 A pseudo-divergence-free field

3.1 Diffuse divergence

In the previous section the diffuse derivative was introduced and its convergence to the actual derivative as $\rho \to 0$ was proven. Incompressible computations require a divergence-free approximating field. That is, the solution $\boldsymbol{u}(\boldsymbol{x})$, now a vector $\boldsymbol{u} : \mathbb{R}^{\mathtt{n_{sd}}} \to \mathbb{R}^{\mathtt{n_{sd}}}$, verifies $\nabla \cdot \boldsymbol{u} = 0$, and the approximation $\boldsymbol{u}^\rho(\boldsymbol{x})$ should also be divergence-free. This condition however depends on the interpolation space. Here, instead of imposing a divergence-free interpolation, the diffuse divergence of the approximation, $\boldsymbol{u}^\rho$, is imposed equal to zero. That is, given an interpolation defined as

$$\boldsymbol{u}^\rho = \begin{pmatrix} u_1^\rho \\ \vdots \\ u_{\mathtt{n_{sd}}}^\rho \end{pmatrix} = \begin{pmatrix} \mathbf{P}^\mathsf{T}\mathbf{a}_1 \\ \vdots \\ \mathbf{P}^\mathsf{T}\mathbf{a}_{\mathtt{n_{sd}}} \end{pmatrix} = \begin{pmatrix} p_0(\boldsymbol{x})\ \mathbf{I}_{\mathtt{n_{sd}}} & \cdots & p_l(\boldsymbol{x})\ \mathbf{I}_{\mathtt{n_{sd}}} \end{pmatrix} \begin{pmatrix} \mathbf{c}_0(\boldsymbol{x}) \\ \vdots \\ \mathbf{c}_l(\boldsymbol{x}) \end{pmatrix} = \mathbf{Q}^\mathsf{T}\mathbf{c}$$

impose

$$\nabla^\delta \cdot \boldsymbol{u}^\rho := \sum_{i=1}^{\mathtt{n_{sd}}} \frac{\delta \boldsymbol{u}^\rho}{\delta x_i} = \sum_{i=1}^{\mathtt{n_{sd}}} \frac{\partial \mathbf{P}^\mathsf{T}}{\partial x_i}\,\mathbf{a}_i(\boldsymbol{x}) = \left(\nabla \cdot \mathbf{Q}^\mathsf{T}(\boldsymbol{x})\right)\mathbf{c}(\boldsymbol{x}) = 0. \tag{19}$$

Note that $\mathbf{I}_{\mathtt{n_{sd}}}$ is the identity matrix of order $\mathtt{n_{sd}}$ and the coefficients have been rearranged as

$$\mathbf{c}^\mathsf{T} = \Big(\underbrace{\mathrm{a}_{0,1}\ \cdots\ \mathrm{a}_{0,\mathtt{n_{sd}}}}_{\mathbf{c}_0^\mathsf{T}(\boldsymbol{x})}\quad \underbrace{\mathrm{a}_{1,1}\ \cdots\ \mathrm{a}_{1,\mathtt{n_{sd}}}}_{\mathbf{c}_1^\mathsf{T}(\boldsymbol{x})}\ \cdots\ \underbrace{\mathrm{a}_{l,1}\ \cdots\ \mathrm{a}_{l,\mathtt{n_{sd}}}}_{\mathbf{c}_l^\mathsf{T}(\boldsymbol{x})}\Big).$$

Equation (19) must hold at each point $\boldsymbol{x}$ and for any approximation. Thus appropriate interpolation functions, $\mathbf{Q}$, must be defined in order to verify (19) and thus ensure asymptotically a divergence-free interpolation (i.e., the divergence-free condition is fulfilled as $\rho \to 0$).

3.2 A 2D pseudo-divergence-free interpolation

The previous concepts are particularized in a 2D case to clearly define pseudo-divergence-free (PDF) interpolation functions. Suppose for instance that consistency of order two is desired, then $\mathbf{P}^{\mathsf{T}} = \{1, x_1, x_2, x_1^2/2, x_1x_2, x_2^2/2\}$, thus

$$\mathbf{Q}^{\mathsf{T}}(\boldsymbol{x}) = \begin{pmatrix} 1 & 0 & x_1 & 0 & x_2 & 0 & x_1^2/2 & 0 & x_1x_2 & 0 & x_2^2/2 & 0 \\ 0 & 1 & 0 & x_1 & 0 & x_2 & 0 & x_1^2/2 & 0 & x_1x_2 & 0 & x_2^2/2 \end{pmatrix} \tag{20}$$

and

$$\mathbf{c}^{\mathsf{T}} = \begin{pmatrix} \mathrm{a}_{0,1} & \mathrm{a}_{0,2} & \mathrm{a}_{1,1} & \mathrm{a}_{1,2} & \mathrm{a}_{2,1} & \mathrm{a}_{2,2} & \mathrm{a}_{3,1} & \mathrm{a}_{3,2} & \mathrm{a}_{4,1} & \mathrm{a}_{4,2} & \mathrm{a}_{5,1} & \mathrm{a}_{5,2} \end{pmatrix}. \tag{21}$$

The PDF condition defined by (19) is, in this case, written as

$$\nabla^{\delta} \cdot \boldsymbol{u}^{\rho} = \frac{\partial \mathbf{P}^{\mathsf{T}}}{\partial x_1}\, \mathbf{a}_1 + \frac{\partial \mathbf{P}^{\mathsf{T}}}{\partial x_2}\, \mathbf{a}_2 = 0,$$

which implies: $(\mathrm{a}_{1,1}+\mathrm{a}_{2,2})+x_1(\mathrm{a}_{3,1}+\mathrm{a}_{4,2})+x_2(\mathrm{a}_{4,1}+\mathrm{a}_{5,2}) = 0$, and consequently,

$$\mathrm{a}_{1,1} + \mathrm{a}_{2,2} = 0, \quad \mathrm{a}_{3,1} + \mathrm{a}_{4,2} = 0, \quad \text{and} \quad \mathrm{a}_{4,1} + \mathrm{a}_{5,2} = 0.$$

The influence of these three restrictions in the interpolation functions (20) can be viewed as follows

$$\begin{pmatrix} 1 & 0 & x_1 & 0 & x_2 & 0 & x_1^2/2 & 0 & x_1x_2 & 0 & x_2^2/2 & 0 \\ 0 & 1 & -x_2 & x_1 & 0 & 0 & -x_1x_2 & x_1^2/2 & -x_2^2/2 & 0 & 0 & 0 \end{pmatrix}, \tag{22}$$

where one should note that the coefficients in the x_1 and x_2 directions are now coupled and that the total number of degrees of freedom has decreased.

3.3 The pseudo-divergence-free EFG method

Using (22), let $\mathbf{Q}_{\delta}$ be the new interpolation matrix (where obviously the unnecessary columns have been removed). The interpolation is then defined as

$$\boldsymbol{u}(\boldsymbol{z}) \simeq \boldsymbol{u}^{\rho}(\boldsymbol{x}, \boldsymbol{z}) = \begin{pmatrix} u_1^{\rho}(\boldsymbol{x}, \boldsymbol{z}) \\ u_2^{\rho}(\boldsymbol{x}, \boldsymbol{z}) \end{pmatrix} = \mathbf{Q}_{\delta}^{\mathsf{T}}(\boldsymbol{z})\ \mathbf{c}(\boldsymbol{x}). \tag{23}$$

The MLS approximation requires to solve at each point $\boldsymbol{x}$ the normal equations, see (3),

$$\mathbf{M}(\boldsymbol{x})\ \mathbf{c}(\boldsymbol{x}) = \sum_{i \in I_{\boldsymbol{x}}} \phi(\boldsymbol{x}, \boldsymbol{x}_i)\ \mathbf{Q}_{\delta}(\boldsymbol{x}_i)\ \boldsymbol{u}(\boldsymbol{x}_i),$$

where

$$\mathbf{M}(\boldsymbol{x}) := \sum_{i \in I_{\boldsymbol{x}}} \phi(\boldsymbol{x}, \boldsymbol{x}_i)\ \mathbf{Q}_\delta(\boldsymbol{x}_i)\ \mathbf{Q}^{\mathsf{T}}{}_\delta(\boldsymbol{x}_i).$$

As previously, the coefficients $\mathbf{c}$ are substituted in (23) and the approximation is particularized at $\boldsymbol{z} = \boldsymbol{x}$. Then, equation (5) becomes

$$\boldsymbol{u}(\boldsymbol{x}) \simeq \boldsymbol{u}^\rho(\boldsymbol{x}) = \mathbf{Q}_\delta^{\mathsf{T}}(\boldsymbol{x})\ \mathbf{c}(\boldsymbol{x}) = \mathbf{Q}_\delta^{\mathsf{T}}(\boldsymbol{x})\ \mathbf{M}^{-1}(\boldsymbol{x}) \sum_{i \in I_{\boldsymbol{x}}} \phi(\boldsymbol{x}, \boldsymbol{x}_i)\ \mathbf{Q}_\delta(\boldsymbol{x}_i)\ \boldsymbol{u}(\boldsymbol{x}_i),$$

and a final expression similar to (6) can be found:

$$\boldsymbol{u}^\rho(\boldsymbol{x}) = \sum_{i \in I_{\boldsymbol{x}}} \mathbf{N}_i^\rho(\boldsymbol{x})\ \boldsymbol{u}(\boldsymbol{x}_i) = \sum_{i \in I_{\boldsymbol{x}}} \Big[\phi(\boldsymbol{x}, \boldsymbol{x}_i)\ \mathbf{Q}_\delta^{\mathsf{T}}(\boldsymbol{x})\ \mathbf{M}^{-1}(\boldsymbol{x})\ \mathbf{Q}_\delta(\boldsymbol{x}_i) \Big] \boldsymbol{u}(\boldsymbol{x}_i).$$

It is important to note that the matrix of interpolation functions $\mathbf{N}_i^\rho$ is now a full matrix, not a diagonal one as standard EFG would induce in this non scalar problem. This is due to the fact that the two components of the solution are linked by the incompressibility restriction.

4 Stationary Stokes problem

The model problem, steady Stokes flow, is used to analyze the performance of the PDF EFG formulation. It is well-known that continuous and discrete spaces for Stokes equations must verify an inf-sup condition [1]. This stability requirement is evidenced in practical computations by the existence of spurious pressure modes. The pseudo-divergence-free velocity field and the pressure field employed should comply asymptotically with the LBB condition.

4.1 Statement of the problem

Let Ω denote an open bounded region of $\mathbb{R}^2$ with boundary $\partial\Omega$. The 2D Stokes problem in Ω seeks a velocity field $\boldsymbol{u} = (u_1, u_2)$ and a pressure field p such that:

$$\begin{cases} -\nu \Delta \boldsymbol{u} + \nabla p = \boldsymbol{f} & \text{in } \Omega, \\ \nabla \cdot \boldsymbol{u} = 0 & \text{in } \Omega, \\ \boldsymbol{u} = \boldsymbol{g} & \text{on } \partial\Omega, \end{cases} \tag{24}$$

where ν is the viscosity of the fluid and $\boldsymbol{f}$ is the body force.

Taking $\boldsymbol{g} = \boldsymbol{0}$, the weak form of the Stokes problem defined in (24) is: find $(\boldsymbol{u}, p) \in \boldsymbol{\mathcal{V}} \times \mathcal{Q}$, where $\boldsymbol{\mathcal{V}} := [\mathcal{H}^1(\Omega)]^2$ and $\mathcal{Q} := \mathcal{L}_2(\Omega)$, such that

$$a(\boldsymbol{u}, \boldsymbol{v}) + b(\boldsymbol{v}, p) + b(\boldsymbol{u}, q) = (\boldsymbol{f}, \boldsymbol{v}) \qquad \forall (\boldsymbol{v}, q) \in \boldsymbol{\mathcal{V}} \times \mathcal{Q}$$

and $\boldsymbol{u} = \boldsymbol{g}$ on $\partial\Omega$, where the bilinear forms $a(\cdot, \cdot)$ and $b(\cdot, \cdot)$ are defined as

$$\begin{aligned} a(\boldsymbol{u}, \boldsymbol{v}) &:= \int_\Omega \nabla \boldsymbol{v} : \nu \nabla \boldsymbol{u} \, d\Omega = \nu(\nabla \boldsymbol{u}, \nabla \boldsymbol{v}), \quad \text{and} \\ b(\boldsymbol{v}, p) &:= -\int_\Omega p \, \nabla \cdot \boldsymbol{v} \, d\Omega \;\; = -(p, \nabla \cdot \boldsymbol{v}). \end{aligned}$$

Note that $(\cdot, \cdot)$ denotes the standard $\mathcal{L}_2(\Omega)$-scalar product.

In order to impose the Dirichlet boundary conditions Nitsche's method [28–32] is used because it produces reasonable results in mesh-free methods and it is more stable than Lagrange multipliers or penalty methods without introducing another discretization on the boundary, see [32] in this same volume for a discussion on imposing Dirichlet boundary conditions in mesh-free methods. Under this circumstances, the weak form becomes

$$\begin{aligned} &a(\boldsymbol{u}, \boldsymbol{v}) + b(\boldsymbol{v}, p) + b(\boldsymbol{u}, q) \\ &\quad - (\nu \partial_{\boldsymbol{n}} \boldsymbol{u} - p \, \boldsymbol{n}, \boldsymbol{v})_{\partial\Omega} - (\boldsymbol{u}, \nu \partial_{\boldsymbol{n}} \boldsymbol{v} - q \, \boldsymbol{n})_{\partial\Omega} + \nu \hat{\gamma} (\boldsymbol{u}, \boldsymbol{v})_{\partial\Omega} \\ &\qquad = (\boldsymbol{f}, \boldsymbol{v}) - (\boldsymbol{g}, \nu \partial_{\boldsymbol{n}} \boldsymbol{v} - q \, \boldsymbol{n})_{\partial\Omega} + \nu \hat{\gamma} (\boldsymbol{g}, \boldsymbol{v})_{\partial\Omega}, \end{aligned} \tag{25}$$

where $\hat{\gamma}$ is not a penalty parameter, but must be large enough to ensure stability. In fact, it is an "arbitrary" (for the convergence analysis point of view) positive value.

We now turn to the consideration of an approximate discrete solution of the problem. Let $\boldsymbol{\mathcal{V}}_\rho$ and $\mathcal{Q}_\rho$ denote finite dimensional subspaces of $\boldsymbol{\mathcal{V}}$ and $\mathcal{Q}$ respectively. The index ρ refers to a characteristic measure of the support of the interpolation functions. It is related to the characteristic measure between particles, h (recall, ρ/h is assumed constant). The discrete version of the problem reads: find $\boldsymbol{u}^\rho \in \boldsymbol{\mathcal{V}}_\rho$ and $p^\rho \in \mathcal{Q}_\rho$ such that, $\forall (\boldsymbol{v}^\rho, q^\rho) \in \boldsymbol{\mathcal{V}}_\rho \times \mathcal{Q}_\rho$,

$$\begin{aligned} &a(\boldsymbol{u}^\rho, \boldsymbol{v}^\rho) + b(\boldsymbol{v}^\rho, p^\rho) + b(\boldsymbol{u}^\rho, q^\rho) \\ &\quad - (\nu \partial_{\boldsymbol{n}} \boldsymbol{u}^\rho - p^\rho \boldsymbol{n}, \boldsymbol{v}^\rho)_{\partial\Omega} - (\boldsymbol{u}^\rho, \nu \partial_{\boldsymbol{n}} \boldsymbol{v}^\rho - q^\rho \boldsymbol{n})_{\partial\Omega} + \nu \frac{\gamma}{\rho} (\boldsymbol{u}^\rho, \boldsymbol{v}^\rho)_{\partial\Omega} \\ &\qquad = (\boldsymbol{f}, \boldsymbol{v}^\rho) - (\boldsymbol{g}, \nu \partial_{\boldsymbol{n}} \boldsymbol{v}^\rho - q^\rho \boldsymbol{n})_{\partial\Omega} + \nu \frac{\gamma}{\rho} (\boldsymbol{g}, \boldsymbol{v}^\rho)_{\partial\Omega}. \end{aligned}$$

Now, $(\cdot, \cdot)_{\partial\Omega}$ denotes the $\mathcal{L}_2(\partial\Omega)$-scalar product. Note that the scalar $\hat{\gamma}$ is replaced by $\hat{\gamma} = \gamma/\rho$ because the threshold of this parameter is inversely

proportional to ρ. To guarantee that γ is large enough an eigenvalue problem is solved, see [33].

5 The PDF formulation and the inf-sup compatibility condition

5.1 The inf-sup condition

The previous problem, see (25), can be written in the following form: find $(\boldsymbol{u}, p) \in \boldsymbol{\mathcal{V}} \times \mathcal{Q}$ such that

$$\begin{cases} A(\boldsymbol{u}, \boldsymbol{v}) + B(\boldsymbol{v}, p) = F(\boldsymbol{v}) & \forall \boldsymbol{v} \in \boldsymbol{\mathcal{V}}, \\ B(\boldsymbol{u}, q) = G(q) & \forall q \in \mathcal{Q}, \end{cases} \tag{26}$$

where the new forms are defined as

$$\begin{aligned} A(\boldsymbol{u}, \boldsymbol{v}) &:= a(\boldsymbol{u}, \boldsymbol{v}) - (\nu \partial_{\boldsymbol{n}} \boldsymbol{u}, \boldsymbol{v})_{\partial\Omega} - (\boldsymbol{u}, \nu \partial_{\boldsymbol{n}} \boldsymbol{v})_{\partial\Omega} + \nu \hat{\gamma} (\boldsymbol{u}, \boldsymbol{v})_{\partial\Omega}, \\ B(\boldsymbol{v}, p) &:= b(\boldsymbol{v}, p) + (p\, \boldsymbol{n}, \boldsymbol{v})_{\partial\Omega}, \\ F(\boldsymbol{v}) &:= (\boldsymbol{f}, \boldsymbol{v}) - (\boldsymbol{g}, \nu \partial_{\boldsymbol{n}} \boldsymbol{v})_{\partial\Omega} + \nu \hat{\gamma} (\boldsymbol{g}, \boldsymbol{v})_{\partial\Omega}, \\ G(q) &:= (\boldsymbol{g}, q\, \boldsymbol{n})_{\partial\Omega}. \end{aligned}$$

The variational problem defined by (26) is well-posed if the following conditions are verified [10]:

i) $A(\cdot, \cdot)$ and $B(\cdot, \cdot)$ are continuous, i.e.,

$$\begin{aligned} &\exists M_1 \text{ such that } \forall \boldsymbol{u} \in \boldsymbol{\mathcal{V}},\ \forall \boldsymbol{v} \in \boldsymbol{\mathcal{V}} && A(\boldsymbol{u}, \boldsymbol{v}) \le M_1 \|\boldsymbol{u}\| \|\boldsymbol{v}\|, \\ &\exists M_2 \text{ such that } \forall \boldsymbol{u} \in \boldsymbol{\mathcal{V}},\ \forall q \in \mathcal{Q} && B(\boldsymbol{v}, q) \le M_2 \|\boldsymbol{v}\| \|q\|. \end{aligned}$$

ii) $A(\cdot, \cdot)$ is coercive, i.e.,

$$\exists \alpha \text{ such that } \forall \boldsymbol{v} \in \boldsymbol{\mathcal{V}}\ A(\boldsymbol{v}, \boldsymbol{v}) \ge \alpha \|\boldsymbol{v}\|^2.$$

iii) $B(\cdot, \cdot)$ satisfies:

$$\inf_{q \in \mathcal{Q}} \sup_{\boldsymbol{v} \in \boldsymbol{\mathcal{V}}} \frac{B(\boldsymbol{v}, q)}{\|\boldsymbol{v}\|\, \|q\|} \ge \beta > 0.$$

Here consideration is given to the discrete problem arising when (26) is discretized using $\boldsymbol{\mathcal{V}}_\rho$ and $\mathcal{Q}_\rho$ finite dimensional subspaces of $\boldsymbol{\mathcal{V}}$ and $\mathcal{Q}$, respectively. The index ρ refers to a characteristic measure of the support of the interpolation functions and it is related to the characteristic measure between particles, h, because, as usual, we assume ρ/h constant. Conditions *i)* and *ii)* carry over to the discrete model and condition *iii)* becomes:

$$\inf_{q^\rho \in \mathcal{Q}_\rho} \sup_{\boldsymbol{v}^\rho \in \boldsymbol{\mathcal{V}}_\rho} \frac{B(\boldsymbol{v}^\rho, q^\rho)}{\|\boldsymbol{v}^\rho\|\, \|q^\rho\|} =: k_\rho > 0. \tag{27}$$

The stability condition needed for the convergence of the discrete model is:

$$\lim_{\rho \to 0} k_\rho \geq \beta > 0.$$

To verify analytically (27) for a given pair $(\mathcal{Q}_\rho, \boldsymbol{\mathcal{V}}_\rho)$ is not trivial. For this reason the numerical inf-sup test allows, with relatively little effort, to indicate whether the inf-sup condition is passed or not.

5.2 The numerical inf-sup test

First, in order to introduce the matrix notation, the discretized problem is recalled: find $\boldsymbol{u}^\rho \in \boldsymbol{\mathcal{V}}_\rho$ and $p^\rho \in \mathcal{Q}_\rho$ such that

$$\begin{cases} A(\boldsymbol{u}^\rho, \boldsymbol{v}^\rho) + B(\boldsymbol{v}^\rho, p^\rho) = F(\boldsymbol{v}^\rho) & \forall \boldsymbol{v}^\rho \in \boldsymbol{\mathcal{V}}_\rho, \\ B(\boldsymbol{u}^\rho, q^\rho) = G(q^\rho) & \forall q^\rho \in \mathcal{Q}_\rho. \end{cases}$$

After discretization, the matrix form is obtained,

$$\begin{pmatrix} \mathbf{A} & \mathbf{B}^\mathsf{T} \\ \mathbf{B} & \mathbf{0} \end{pmatrix} \begin{pmatrix} \mathbf{u} \\ \mathbf{p} \end{pmatrix} = \begin{pmatrix} \mathbf{F} \\ \mathbf{G} \end{pmatrix}$$

where $\mathbf{A}$ and $\mathbf{B}$ are the matrices associated to the bilinear forms $A(\cdot, \cdot)$ and $B(\cdot, \cdot)$ respectively.

The numerical inf-sup test is based in the next theorem.

Proposition 2 *Let $\mathbf{M}_{\boldsymbol{v}}$ and $\mathbf{M}_q$ be the mass matrices associated to the scalar products of $\boldsymbol{\mathcal{V}}_\rho$ and $\mathcal{Q}_\rho$ respectively and let μ_{min} be the smallest non zero eigenvalue defined by the following eigenproblem:*

$$\mathbf{B}^\mathsf{T} \mathbf{M}_q^{-1} \mathbf{B} \boldsymbol{v} = \mu^2 \mathbf{M}_{\boldsymbol{v}} \boldsymbol{v}$$

then the value of k_ρ is simply $\mu_{\min}$.

The proof can be found in [9] or [10]. The numerical test proposed in [11] consists in testing a particular formulation by calculating k_ρ using meshes of increasing refinement. On the basis of three or four results it can be predicted whether the inf-sup value is probably bounded from underneath or, on the contrary, goes down to zero when the mesh is refined. The good behavior of this test is demonstrated on several examples of elements for the incompressible elasticity problem in [11]. In the following section this test is used to check the behavior of the proposed PDF EFG method.

5.3 Numerical test of the PDF EFG method

In order to perform the numerical inf-sup test a sequence of four successive refined meshes is considered (uniform distributions of 11×11, 21×21, ..., 81×81 particles). The objective is to monitor the inf-sup values, k_ρ, when h decreases. Remember that the dilation parameter, ρ/h, is kept constant, and thus, if h decreases ρ also decreases.

If a steady decrease in $\log(k_\rho)$ is observed when h goes to zero, the element is predicted to violate the inf-sup condition and said to fail the numerical test. But, if the $\log(k_\rho)$ stabilizes as the number of particles (or elements) increases, the test is passed.

Figure 1 shows numerical tests comparing the finite element method (FEM), the standard element free Galerkin method (EFG) and the pseudo-divergence-free (PDF) EFG method. For each case different mixed interpolations have been employed and compared. Note that some curves present rate of decrease close 1 in the log/log graph, clearly indicating that the numerical inf-sup condition fails. As expected, the finite element interpolations indicate that $Q1P0$, $Q1Q1$ and $Q2Q2$ elements do not verify the inf-sup condition and the $Q2Q1$ element (biquadratic interpolation for velocity and bilinear for pressure) is LBB compliant. Standard EFG method does not improve the finite element results, in fact, the $Q2Q1$ also fails to pass the inf-sup condition. Finally, for the PDF EFG method $\log(k_\rho)$ appears to be bounded in every case.

6 Numerical examples

6.1 Analytical test

In order to illustrate the behavior of the PDF EFG interpolation in the solution of stationary Stokes flow we consider a two-dimensional problem in the square domain $\Omega =]0,1[\times]0,1[$, which possesses a closed-form analytical solution [34]. The problem consists of determining the velocity field $\boldsymbol{u} = (u_1, u_2)$ and the pressure p such that

$$\begin{cases} -\nu\Delta\boldsymbol{u} + \nabla p = \boldsymbol{f} & \text{in } \Omega, \\ \nabla \cdot \boldsymbol{u} = 0 & \text{in } \Omega, \\ \boldsymbol{u} = 0 & \text{on } \partial\Omega, \end{cases}$$

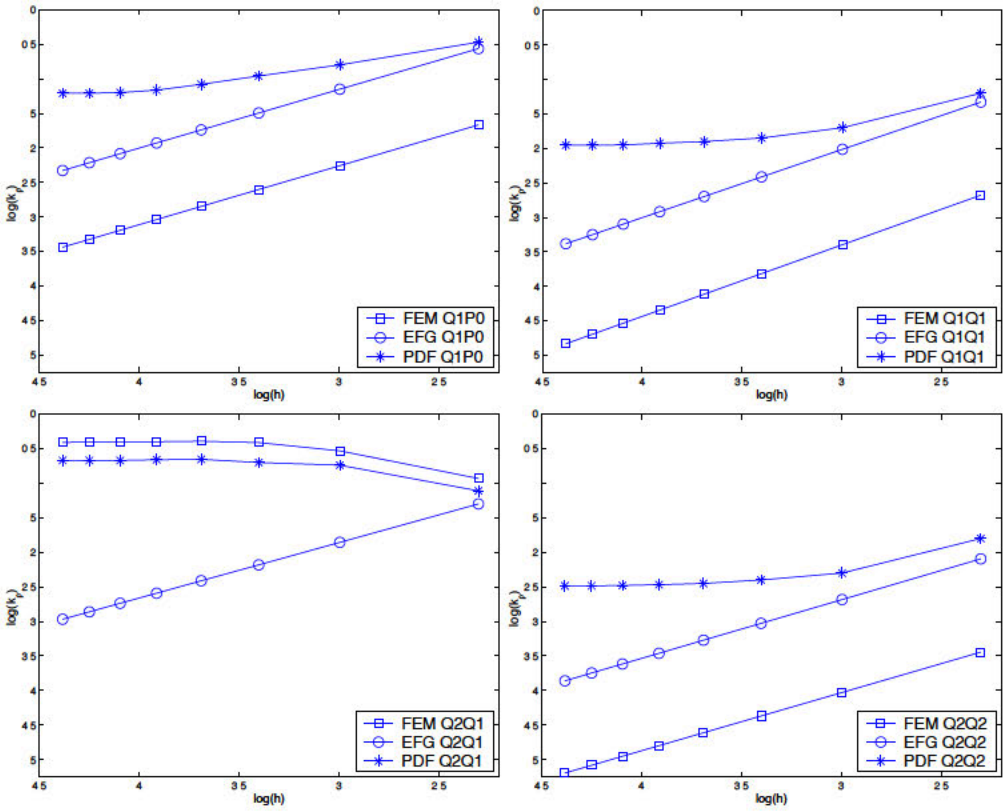

Fig. 1. Inf-sup results: comparing FEM, EFG and the PDF EFG method.

where the fluid viscosity is taken as $\nu = 1$. The components of the body force $\boldsymbol{f}$ are prescribed as

$$
\begin{aligned}
f_1 = {} & (12 - 24\,y)\,x^4 + (-24 + 48\,y)\,x^3 + (-48\,y + 72\,y^2 - 48\,y^3 + 12)\,x^2 \\
& + (-2 + 24\,y - 72\,y^2 + 48\,y^3)\,x + 1 - 4\,y + 12\,y^2 - 8\,y^3, \\
f_2 = {} & (8 - 48\,y + 48\,y^2)\,x^3 + (-12 + 72\,y - 72\,y^2)\,x^2 \\
& + (4 - 24\,y + 48\,y^2 - 48\,y^3 + 24\,y^4)\,x - 12\,y^2 + 24\,y^3 - 12\,y^4,
\end{aligned}
$$

where, for simplicity, we have used in this 2D problem the notation $(x, y) := (x_1, x_2)$. With this prescribed body force, the exact solution is

$$
\begin{aligned}
u_1(x, y) = {} & \quad x^2\,(1 - x)^2\,(2\,y - 6\,y^2 + 4\,y^3), \\
u_2(x, y) = {} & -y^2\,(1 - y)^2\,(2\,x - 6\,x^2 + 4\,x^3), \\
p(x, y) = {} & \; x\,(1 - x).
\end{aligned}
$$

This problem is solved with the standard EFG and the PDF EFG method using $\rho/h = 1.2$ with an equal bilinear interpolation base for velocity and pressure, the results are shown in Figures 2 and 3. Note that, on one hand, standard EFG produces, as expected, unstable pressure results (and a reasonable velocity field). On the other hand, the PDF EFG results are stable and no spurious global oscillations are observed on the pressure field.

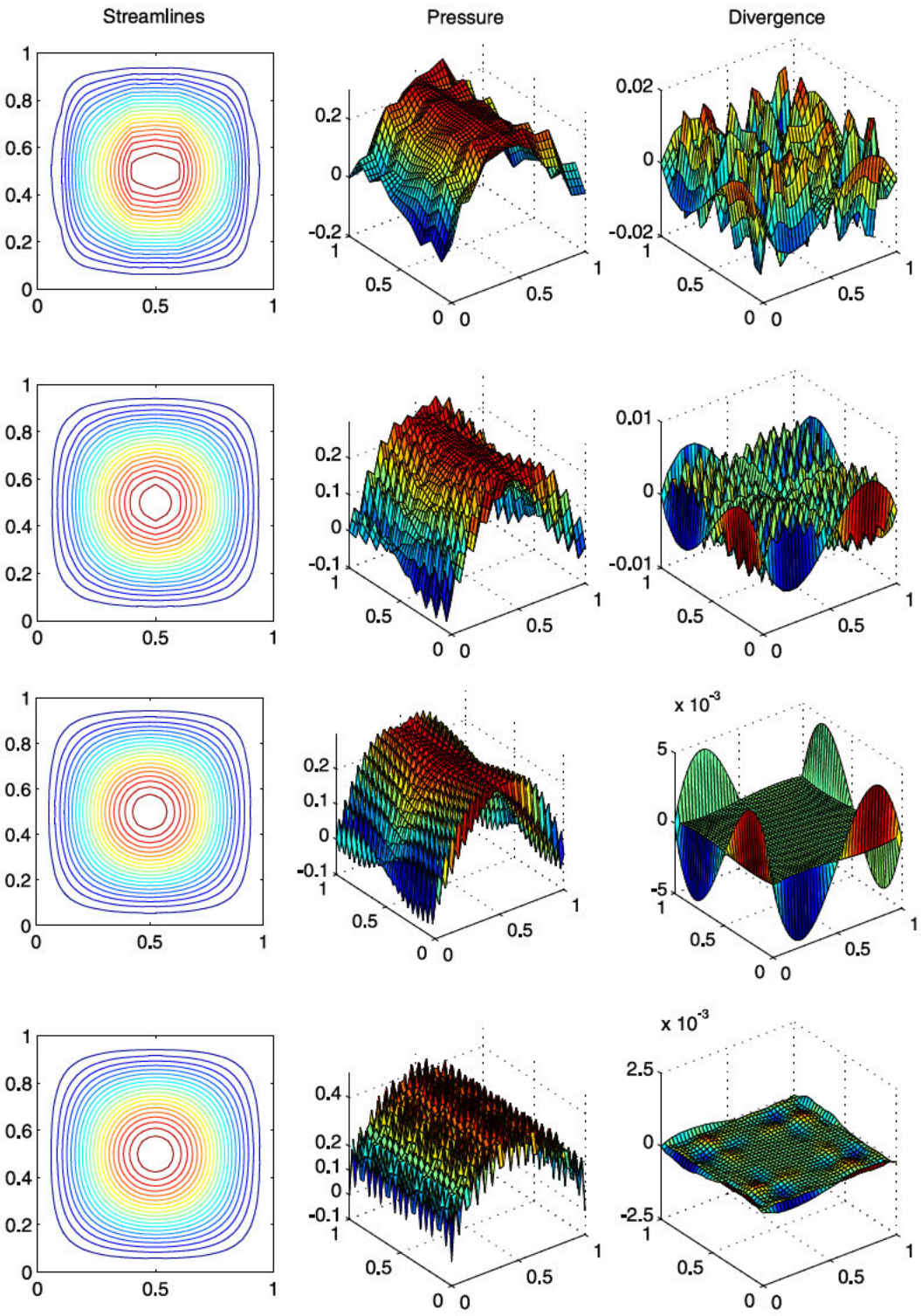

Fig. 2. Stokes problem with analytical solution: results for standard EFG and a uniform distribution of particles, from top to bottom 11×11, 21×21, 41×41 and 81×81.

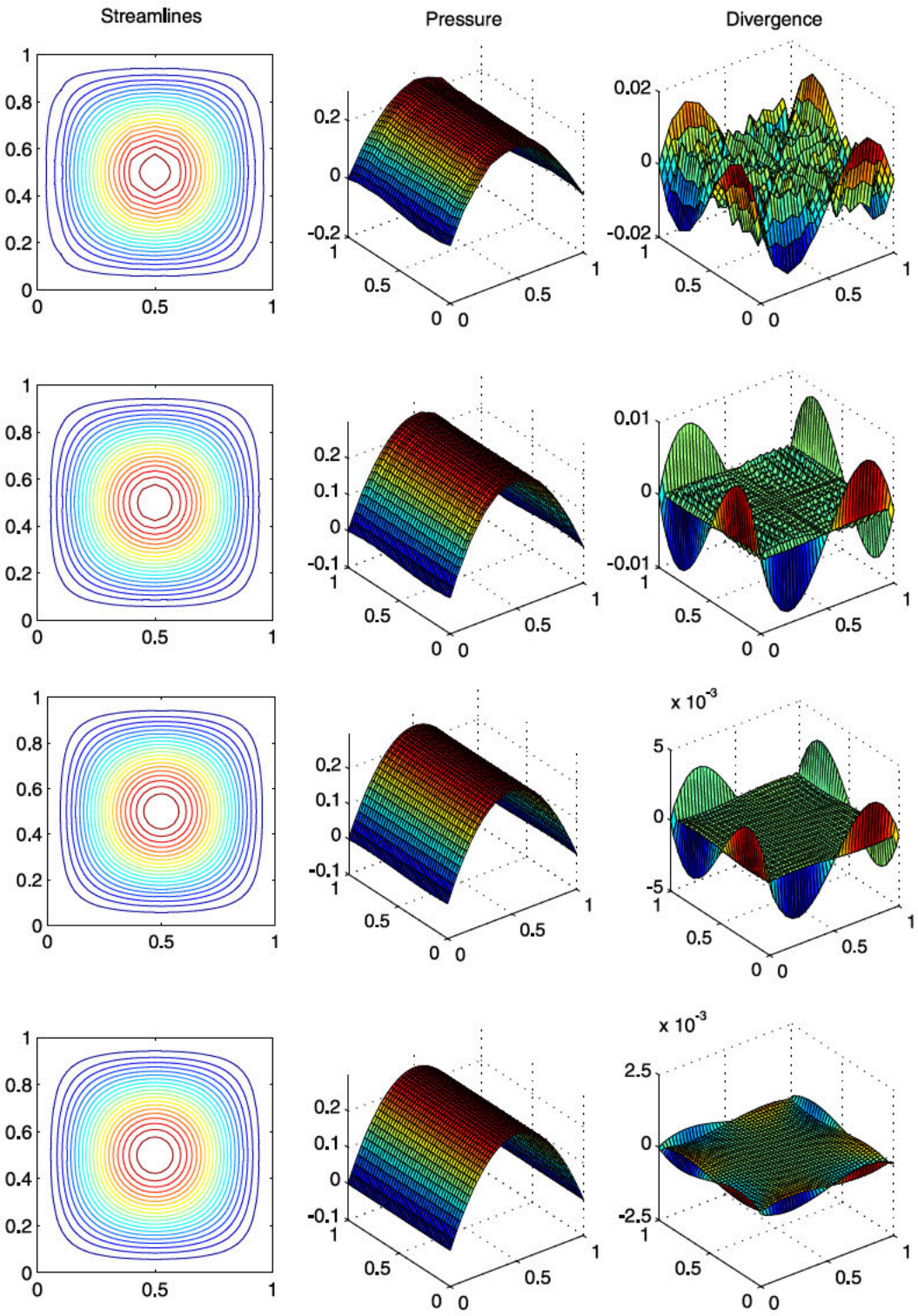

Fig. 3. Stokes problem with analytical solution: results for pseudo-divergence-free (PDF) EFG and a uniform distribution of particles, from top to bottom 11×11, 21×21, 41×41 and 81×81.

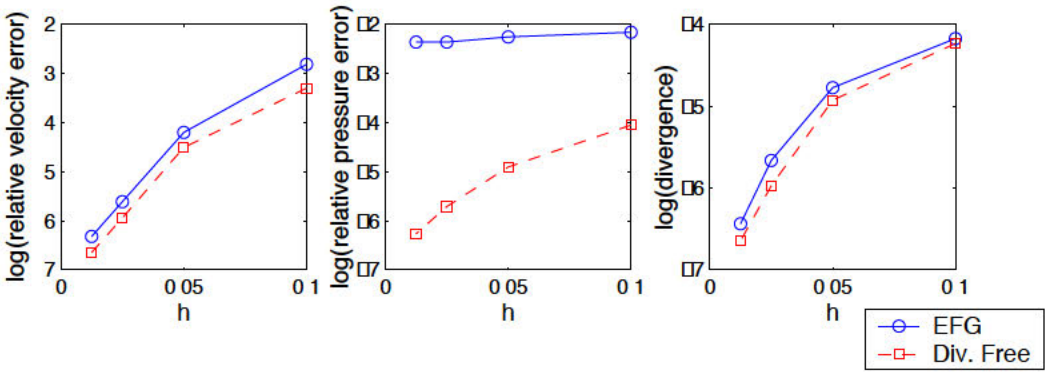

Fig. 4. Stokes problem with analytical solution: convergence results for velocities (left), pressures (middle) and divergence (right).

These observations are corroborated by the convergence results, which are shown in Figure 4. The velocity convergence rates for standard EFG and for the PDF method are, as expected, similar. However, convergence in pressure is far from optimal in EFG, whereas it presents the theoretical slope in the proposed approach. Recall that equation (8) indicates that diffuse derivatives converge to the actual derivatives as $\rho \to 0$ ($\rho/h = \text{cst}$). Since we use a bilinear base (i.e. $m = 1$) the convergence behaves as ρ^1. This means that if we double the number of particles (i.e., if we divide ρ by 2) then the divergence must be at least divided by two. Figure 4 shows exactly this behavior.

6.2 Driven cavity flow problem

This example has become a standard benchmark test for incompressible flows. We will show here results for the Stokes problem. It models a plane flow of an isothermal fluid in a square lid-driven cavity. The upper side of the cavity moves in its own plane at unit speed, while the other sides are fixed. The domain is $\Omega =]0,1[\times]0,1[$, the body forces are neglected, $\boldsymbol{f} = (0,0)^\mathsf{T}$, and the boundary conditions are formally defined as: $\boldsymbol{g} = (0,0)^\mathsf{T}$ on $\partial\Omega \setminus \{y = 1\}$ and $\boldsymbol{g} = (1,0)^\mathsf{T}$ on $\partial\Omega \cap \{y = 1\}$.

We solve this well-known benchmark problem using $\rho/h = 2.1$ and an equal biquadratic interpolation base to approximate velocity and pressure. Streamlines, pressure distribution and divergence of $\boldsymbol{u}$ are depicted in Figures 5 and 6 for standard EFG and the PDF EFG method, respectively. EFG presents oscillations on the pressure field. Nevertheless, for the PDF approach reasonable results are obtained in spite of the equal order interpolation for velocity and pressure. No spurious pressure modes are observed.

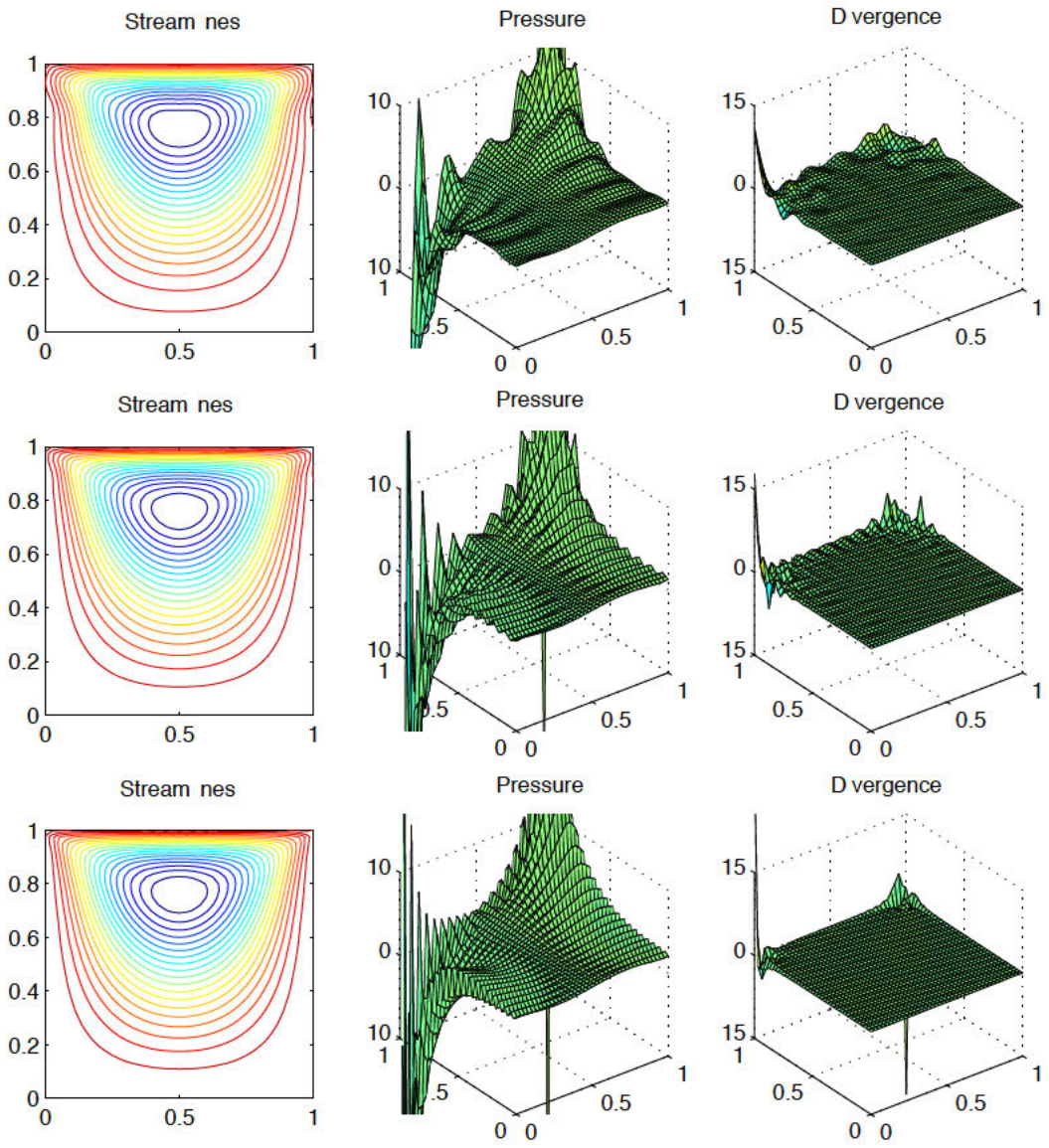

Fig. 5. Standard EFG solution for a uniform distribution of 11×11 (top), 21×21 (middle) and 41×41 (bottom) particles.

7 Conclusions

Mesh-free methods for incompressible materials usually follow the path of finite elements. Here we exploit the advantages of the diffuse derivative to introduce an interpolation space that approaches a divergence-free space in the limit as the discretization is refined.

The pseudo-divergence-free (PDF) EFG method does not require extra computations given a particle distribution, thus the computational overhead is negligible. In fact, only the interpolating polynomials are modified compared with standard EFG. Note that the diffuse derivative is only used to define a

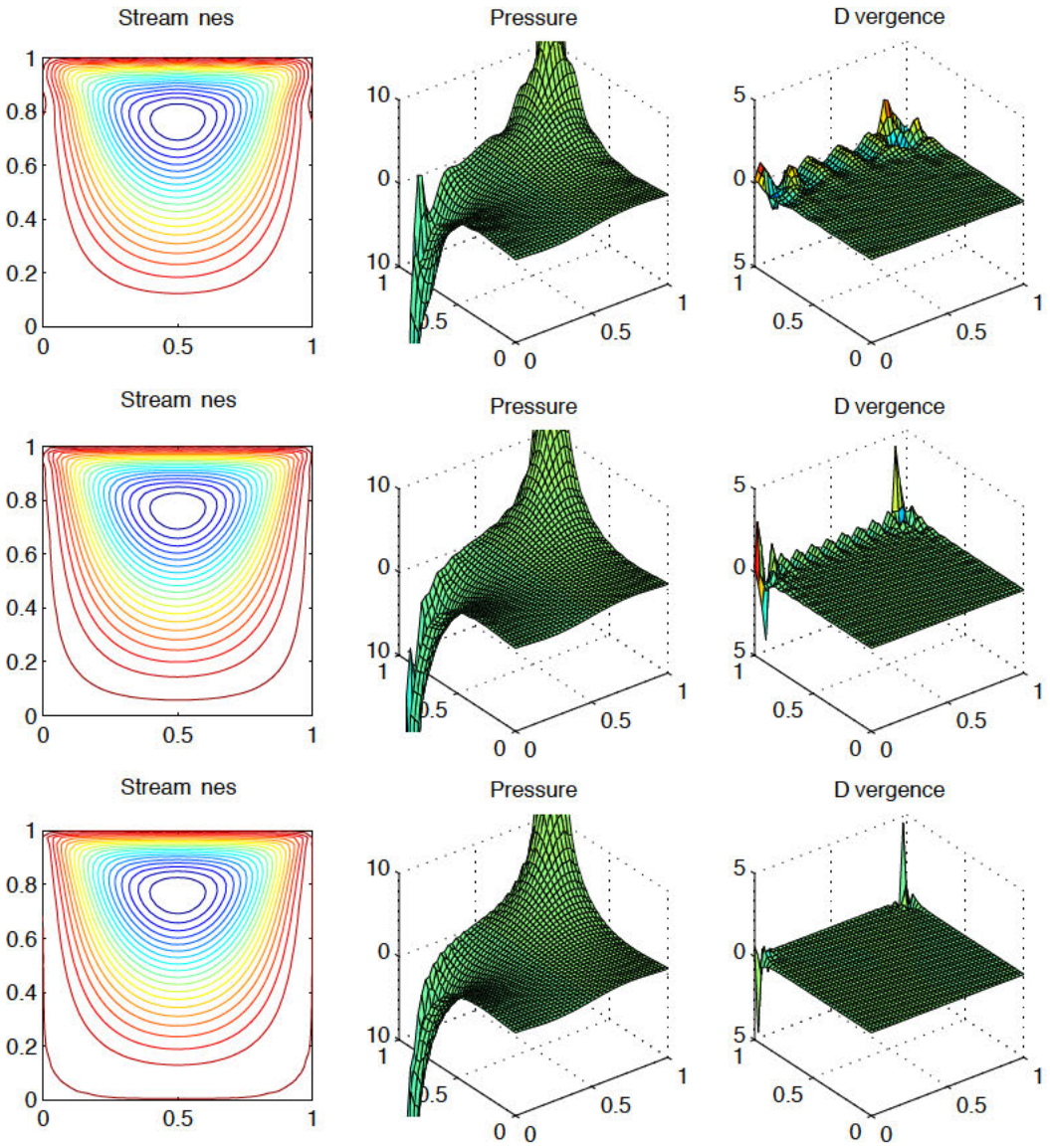

Fig. 6. PDF EFG solution for a uniform distribution of 11x11 (top), 21x21 (middle) and 41x41 (bottom) particles.

priori the interpolation polynomials and that full derivatives (not diffuse ones) are employed in the Galerkin weak forms.

The comparison with standard EFG is clear. EFG fails the numerical inf-sup test for any combination of interpolating spaces in a mixed formulation (also for the $Q2Q1$ that is stable in FEM). However, the PDF EFG allows any combination of interpolating spaces and stability is observed as refinement progresses. Moreover, two well-known benchmark examples for Stokes flow, one with analytical solution and the cavity problem, corroborate these conclusions.

References

[1] V. Girault, P.-A. Raviart, Finite element methods for Navier-Stokes equations. Theory and algorithms, Springer-Verlag, Berlin, 1986.

[2] P. M. Gresho, R. L. Sani, Incompressible flow and the finite element method. Vol. 1: Advection diffusion. Vol. 2: Isothermal laminar flow, John Wiley & Sons, Chichester, 2000.

[3] M. D. Gunzburger, Finite element methods for viscous incompressible flows. A guide to theory, practice, and algorithms, Academic Press, Boston, MA, 1989.

[4] O. Pironneau, Finite element methods for fluids, John Wiley & Sons, Chichester, 1989.

[5] L. Quartapelle, Numerical solution of the incompressible Navier-Stokes equations, Vol. 113 of International Series of Numerical Mathematics, Birkhäuser-Verlag, Basel, 1993.

[6] A. Quarteroni, A. Valli, Numerical Approximation of Partial Differential Equations, Vol. 23 of Springer Series in Computational Mathematics, Springer-Verlag, Berlin, 1994.

[7] R. Temam, Navier-Stokes equations. Theory and numerical analysis, AMS Chelsea Publishing, Providence, RI, 2001, corrected reprint of the 1984 edition [North-Holland, Amsterdam, 1984].

[8] J. Donea, A. Huerta, Finite element methods for flow problems, John Wiley & Sons, Chichester, 2003.

[9] D. S. Malkus, Eigenproblems associated with the discrete LBB condition for incompressible finite elements, Int. J. Eng. Sci. 19 (10) (1981) 1299–1310.

[10] F. Brezzi, M. Fortin, Mixed and hybrid finite element methods, Vol. 15 of Springer Series in Computational Mathematics, Springer-Verlag, New York, 1991.

[11] D. Chapelle, K.-J. Bathe, The inf-sup test, Comput. Struct. 47 (4–5) (1993) 537–545.

[12] K.-J. Bathe, D. Hendriana, F. Brezzi, G. Sangalli, Inf-sup testing of upwind methods, Int. J. Numer. Methods Eng. 48 (5) (2000) 745–760.

[13] T. Zhu, S. N. Atluri, A modified collocation method and a penalty formulation for enforcing the essential boundary conditions in the element free Galerkin method, Comput. Mech. 21 (3) (1998) 211–222.

[14] J. Dolbow, T. Belytschko, Volumetric locking in the element free Galerkin method, Int. J. Numer. Methods Eng. 46 (6) (1999) 925–942.

[15] H. Askes, R. de Borst, O. Heeres, Conditions for locking-free elasto-plastic analyses in the element-free galerkin method, Comput. Methods Appl. Mech. Eng. 173 (1–2) (1999) 99–109.

[16] J. S. Chen, S. Yoon, H. Wang, W. K. Liu, An improved reproducing kernel particle method for nearly incompressible finite elasticity, Comput. Methods Appl. Mech. Eng. 181 (1–3) (2000) 117–145.

[17] T. J. R. Hughes, The finite element method: linear static and dynamic finite element analysis, Dover Publications Inc., New York, 2000, corrected reprint of the 1987 original [Prentice-Hall Inc., Englewood Cliffs, N.J.].

[18] A. Huerta, S. Fernández-Méndez, Locking in the incompressible limit for the element free galerkin method, Int. J. Numer. Methods Eng. 51 (11) (2001) 1361–1383.

[19] B. Nayroles, G. Touzot, P. Villon, Generating the finite element method: diffuse approximation and diffuse elements, Comput. Mech. 10 (5) (1992) 307–318.

[20] P. Villon, Contribution à l'optimisation, Thèse présentée pour l'obtention du grade de docteur d'état, Université de Technologie de Compiègne, Compiègne, France (1991).

[21] Y. Vidal, P. Villon, A. Huerta, Locking in the incompressible limit: pseudo-divergence-free element-free galerkin, Revue européene des éléments finis 11 (7/8) (2002) 869–892.

[22] Y. Vidal, P. Villon, A. Huerta, Locking in the incompressible limit: pseudo-divergence-free element-free galerkin, Commun. Numer. Methods Eng. 19 (9) (2003) 725–735.

[23] W. K. Liu, T. Belytschko, J. T. Oden, editors, Meshless methods, Comput. Methods Appl. Mech. Eng. 139 (1–4) (1996) 1–440.

[24] S. Fernández-Méndez, A. Huerta, Coupling finite elements and particles for adaptivity: An application to consistently stabilized convection-diffusion, in: M. Griebel, M. A. Schweitzer (Eds.), Meshfree methods for partial differential equations, Vol. 26 of Lecture Notes in Computational Science and Engineering, Springer-Verlag, Berlin, 2002, pp. 117–129, papers from the International workshop, Universität Bonn, Germany, September 11-14, 2001.

[25] S. Fernández-Méndez, P. Díez, A. Huerta, Convergence of finite elements enriched with meshless methods, Numer. Math. DOI 10.1007/s00211-003-0465-x.

[26] T. Belytschko, Y. Krongauz, M. Fleming, D. Organ, W. K. Liu, Smoothing and accelerated computations in the element free Galerkin method, J. Comput. Appl. Math. 74 (1–2) (1996) 111–126.

[27] A. Huerta, S. Fernández-Méndez, P. Díez, Enrichissement des interpolations d´ éléments finis en utilisant des méthodes de particules, ESAIM-Math. Model. Numer. Anal. 36 (6) (2002) 1027–1042.

[28] R. Stenberg, On some techniques for approximating boundary conditions in the finite element method, J. Comput. Appl. Math. 63 (1-3) (1995) 139–148.

[29] D. N. Arnold, F. Brezzi, B. Cockburn, L. D. Marini, Unified analysis of discontinuous Galerkin methods for elliptic problems, SIAM J. Numer. Anal. 39 (5) (2001/02) 1749–1779.

[30] I. Babuska, U. Banerjee, J. E. Osborn, Meshless and generalized finite element methods: A survey of some major results, in: M. Griebel, M. A. Schweitzer (Eds.), Meshfree methods for partial differential equations, Vol. 26 of Lecture Notes in Computational Science and Engineering, Springer-Verlag, Berlin, 2002, pp. 1–20, papers from the International workshop, Universität Bonn, Germany, September 11-14, 2001.

[31] R. Becker, Mesh adaptation for dirichlet flow control via nitsche's method, Commun. Numer. Methods Eng. 18 (9) (2002) 669–680.

[32] S. Fernández-Méndez, A. Huerta, Imposing essential boundary conditions in mesh-free methods, Comput. Methods Appl. Mech. Eng. Accepted for publication.

[33] M. Griebel, M. A. Schweitzer, A particle-partition of unity method. Part V: Boundary conditions, in: S. Hildebrandt, H. Karcher (Eds.), Geometric Analysis and Nonlinear Partial Differential Equations, Springer, Berlin, 2002, pp. 517–540.

[34] J. T. Oden, O.-P. Jacquotte, Stability of some mixed finite element methods for Stokesian flows, Comput. Methods Appl. Mech. Eng. 43 (2) (1984) 231–247.